Intermediate-valent Cerium in $CeRu_2Mg_5$

Stefan Linsinger, Matthias Eul, Ute Ch. Rodewald, and Rainer Pöttgen

Institut für Anorganische und Analytische Chemie, Universität Münster, Corrensstraße 30, 48149 Münster, Germany

Reprint requests to R. Pöttgen. E-mail: pottgen@uni-muenster.de

Z. Naturforsch. **2010**, *65b,* 1185 – 1190; received June 25, 2010

The magnesium-rich compound $CeRu_2Mg_5$ was synthesized by high-frequency melting of the elements in a sealed tantalum ampoule. $CeRu_2Mg_5$ crystallizes with a new tetragonal structure type: $P4_2/ncm$, $a = 961.1(1)$, $c = 723.2(1)$ pm, $wR2 = 0.0284$, 481 F^2 values and 25 variables. The striking structural motifs in $CeRu_2Mg_5$ are short Ce–Ru distances of 232 pm. Each cerium atom is connected to two ruthenium atoms within a three-dimensional $[Ru_2Mg_5]$ network. $CeRu_2Mg_5$ has a pronounced magnesium substructure with short Mg–Mg distances in the range 302 – 341 pm. The short Ce–Ru distances are a consequence of the almost tetravalent character of the cerium atoms. Temperature-dependent magnetic susceptibility data show intermediate-valent behavior of the cerium atoms (0.9(1) μ_B per formula unit) and no magnetic ordering down to 3 K.

Key words: Intermetallics, Cerium, Magnesium, Intermediate Valence

Introduction

Intermetallic $Ce_xT_yX_z$ cerium compounds (T = transition metal; X = element of the 3rd, 4th, or 5th main group) are a fascinating class of materials, since the different electronic states of cerium, *i. e.* diamagnetic Ce^{IV} ([Xe] $4f^0$), paramagnetic Ce^{III} ([Xe] $4f^1$) or an intermediate valence lead to a variety of magnetic properties. These phenomena are believed to arise due to hybridization between the $4f$(Ce) electrons and the conduction electrons.

Within this large family of compounds, a peculiar bonding situation arises for T = Ru. Several compounds exhibit unusually short Ce–Ru distances, some of them as short as 228 pm, much shorter than the sum of the covalent radii. This phenomenon has first been observed for the indides $CeRu_{0.88}In_2$, $Ce_{16}Ru_8In_{37}$, $Ce_2Ru_2In_3$, $Ce_3Ru_2In_2$, and $Ce_3Ru_2In_3$ [1 – 5] and recently for CeRuSn [6, 7], Ce_2RuZn_4 [8, 9], $Ce_{23}Ru_7X_4$ (X = Mg, Cd) [10, 11], $CeRu_4B_4$ [12], and CeRuAl [13]. Such short Ce–Ru distances can only be realized with a small, *i. e.* almost tetravalent cerium. Depending on the crystal structure these cerium compounds contain one or more crystallographically independent cerium sites. If only one cerium site is present, the compound shows intermediate cerium valence, while a static ordering of trivalent and intermediate-valent cerium is possible in the case of multiple cerium sites, *e. g.* in CeRuSn [6, 7], Ce_2RuZn_4 [8, 9], and $Ce_{23}Ru_7X_4$ (X = Mg, Cd) [10, 11]. This behavior has been proven by magnetic susceptibility data. Especially the structures of CeRuSn [6] and Ce_2RuZn_4 [8] give unambiguous evidence for $Ce^{III}/Ce^{\sim IV}$ ordering. Electronic structure calculations revealed very strong Ce–Ru bonding for the $Ce^{\sim IV}$ sites.

Bearing these peculiar structural features and unusual magnetic properties in mind, we started systematic phase analytical studies of the Ce–Ru–X systems. In continuation of our investigations of $RE_xT_yMg_z$ intermetallics [14, and refs. therein], we screened the Ce–Ru–Mg system by X-ray powder diffraction and metallography in combination with EDX. So far, only the rare earth metal-rich phases $Ce_{23}Ru_7Mg_4$ [11] and Ce_4RuMg [15] have been characterized. They already contain short Ce–Ru contacts. Herein we report on the structure and magnetic properties of the new magnesium-rich compound $CeRu_2Mg_5$. This phase had first been observed as a minority component during metallographic studies. After the structure determination the phase could be obtained as X-ray-pure bulk material.

Experimental Section

Synthesis

Starting materials for the preparation of $CeRu_2Mg_5$ were a cerium ingot (Sigma Aldrich), ruthenium powder (Allgemeine Gold- und Silberscheideanstalt Pforzheim,

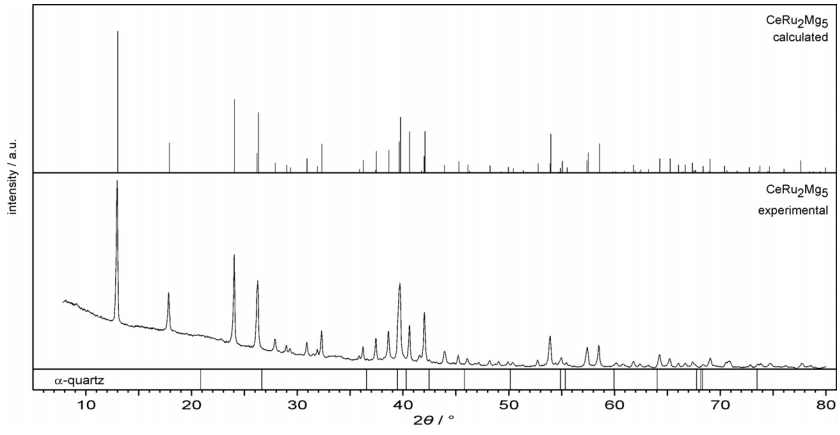

Fig. 1. Experimental (bottom) and calculated (top) Guinier powder diagram (Cu$K_{\alpha 1}$ radiation) of $CeRu_2Mg_5$.

$>$ 99.99 %) and a magnesium rod (Alpha Aesar, $>$ 99.8 %; the surface layer of the rod was removed on a turning lathe). The cerium ingot was first cut into smaller pieces and arc-melted [16] to a small button under an argon atmosphere. The argon was purified with titanium sponge (900 K), silica gel, and molecular sieves. The elements were weighed in the ideal 1 : 2 : 5 atomic ratios and sealed in a tantalum tube under an argon pressure of 700 mbar in an arc melting apparatus. The tantalum tube was subsequently placed in the water-cooled sample chamber of an induction furnace [17] (Hüttinger Elektronik, Freiburg, Germany, Typ TIG 2.5/300), heated to 1373 K, and kept at that temperature for 10 min. Finally, the temperature was lowered to 773 K, and the sample was annealed at that temperature for another 8 h and then cooled within the furnace after the power was switched off. The temperature was controlled by a Sensor Therm Methis MS09 pyrometer with an accuracy of $\pm$30 K. The brittle $CeRu_2Mg_5$ sample could readily be separated from the tantalum tube by mechanical fragmentation. No reaction with the crucible material was evident. $CeRu_2Mg_5$ is stable in air over several weeks. Single crystals exhibit metallic luster while the ground powder is dark grey.

EDX data

Semiquantitative EDX analyses of the $CeRu_2Mg_5$ crystals investigated on the diffractometer and of the bulk sample were carried out by use of a Zeiss EVO MA10 scanning electron microscope with CeO_2, Ru, and MgO as standards. The crystal mounted on a quartz fibre was first coated with a thin carbon film to ensure conductivity. The bulk sample was previously embedded in a methylmetacrylate matrix, and the surface was polished with different silica and diamond pastes. The surface remained unetched for the EDX measurements. The experimentally observed compositions were close to the ideal one. No impurity elements heavier than sodium (detection limit of the instrument) were found.

Table 1. Crystal data and structure refinement for $CeRu_2Mg_5$, space group $P4_2/ncm$, $Z = 4$.

Empirical formula	$CeRu_2Mg_5$
Crystal size, μm^3	$20 \times 30 \times 90$
Unit cell dimensions (Guinier data)	
a, pm	961.1(1)
c, pm	723.2(1)
Cell volume, nm^3	0.6680
Molar mass, g mol^{-1}	463.81
Calculated density, g cm^{-3}	4.61
Transm. ratio (max / min)	0.741 / 0.495
Absorption coefficient, mm^{-1}	11.5
Detector distance, mm	90
Exposure time, min	3
ω range; increment, deg	0 – 180, 1.0
Integr. param. A, B, EMS	12.8; 3.2; 0.012
$F(000)$, e	824
θ range for data collection, deg	3 – 29
Range in hkl	$\pm$12, $\pm$12, $\pm$9
Total no. reflections	4719
Independent reflections / R_{int}	481 / 0.0767
Reflections with $I \geq 2\sigma(I)$ / R_σ	320 / 0.0877
Data / ref. parameters	481 / 25
Goodness-of-fit on F^2	0.520
$R1$ / $wR2$ for $I \geq 2\sigma(I)$	0.0212 / 0.0238
$R1$ / $wR2$ for all data	0.0570 / 0.0284
Extinction coefficient	0.00047(7)
Largest diff. peak / hole, e $Å^{-3}$	0.91 / −1.01

X-Ray diffraction

The $CeRu_2Mg_5$ sample was characterized by a Guinier pattern (imaging plate detector, Fujifilm BAS-1800 readout system) with Cu$K_{\alpha 1}$ radiation and α-quartz (a = 491.30 and c = 540.46 pm) as the internal standard. The tetragonal lattice parameters (Table 1) were refined by a least-squares routine. Correct indexing was ensured through an intensity calculation [18] taking the atomic positions from the structure refinement. The experimental and calculated patterns are compared in Fig. 1.

Table 2. Atomic coordinates and anisotropic displacement parameters (pm^2) for $CeRu_2Mg_5$. U_{eq} is defined as one third of the trace of the orthogonalized U_{ij} tensor. The anisotropic displacement factor exponent takes the form: $-2\pi^2[(ha^*)2U_{11} + \ldots + 2hka^*b^*U_{12}]$.

Atom	W. position	x	y	z	U_{11}	U_{22}	U_{33}	U_{23}	U_{13}	U_{12}	U_{eq}
Ce	4*e*	1/4	1/4	0.43098(8)	104(2)	U_{11}	102(2)	0	0	−16(4)	104(1)
Ru	8*i*	0.08641(4)	x	0.34069(8)	90(2)	U_{11}	100(2)	−3(2)	U_{23}	−4(2)	94(1)
Mg1	4*d*	0	0	0	141(12)	U_{11}	76(14)	−20(9)	U_{23}	−30(16)	119(8)
Mg2	16*j*	0.2016(2)	0.5495(2)	0.1518(2)	120(8)	136(9)	152(7)	−10(8)	−7(7)	15(6)	136(4)

Table 3. Interatomic distances (pm) in the structure of $CeRu_2Mg_5$, calculated with the powder lattice parameters. Standard deviations are given in parentheses.

Ce:	2	Ru	231.7(1)	Mg1:	2	Ru	272.9(1)
	4	Mg2	332.4(2)		4	Mg2	310.8(2)
	2	Mg1	343.5(1)		4	Mg2	321.3(2)
	4	Mg2	354.7(2)		2	Ce	343.5(1)
	2	Ce	361.6(1)	Mg2:	1	Ru	278.0(2)
Ru:	1	Ce	231.7(1)		1	Ru	279.1(2)
	1	Mg1	273.0(1)		1	Ru	282.7(2)
	2	Mg2	278.0(2)		1	Mg2	301.5(3)
	2	Mg2	279.1(2)		1	Mg1	310.8(2)
	2	Mg2	282.7(2)		2	Mg2	314.4(3)
					1	Mg1	321.3(2)
					1	Ce	332.4(2)
					1	Mg2	341.2(3)
					1	Ce	354.7(2)

Small single crystals of $CeRu_2Mg_5$ were selected from the crushed annealed sample. The quality of the crystals was checked by Laue photographs on a Buerger camera (white Mo radiation). Intensity data were collected at room temperature by use of a Stoe IPDS-II imaging plate diffractometer in oscillation mode (graphite-monochromatized MoK_α radiation). A numerical absorption correction was applied to the data set. All relevant details concerning the data collection and evaluation are listed in Table 1.

Structure refinement

Careful analyses of the diffractometer data set revealed the same tetragonal primitive cell as determined from the powder X-ray data. The data set had high Laue symmetry, and the systematic extinctions were compatible with the space group $P4_2/ncm$. The starting atomic parameters were then determined *via* Direct Methods with SHELXS-97 [19], and the structure was refined with anisotropic atomic displacement parameters for all sites using SHELXL-97 [20] (full-matrix least-squares on F^2). As a check for the correct composition, the occupancy parameters were refined in a separate series of least-squares cycles. All sites were fully occupied within two standard deviations and in the final cycles the ideal values were assumed again. The final difference Fourier synthesis was flat (Table 1). The positional parameters and interatomic distances are listed in Tables 2 and 3.

Further details of the crystal structure investigation may be obtained from Fachinformationszentrum Karlsruhe, 76344 Eggenstein-Leopoldshafen, Germany (fax: +49-7247-808-666; e-mail: crysdata@fiz-karlsruhe.de, http://www.fiz-informationsdienste.de/en/DB/icsd/depot_anforderung.html) on quoting the deposition number CSD-421908.

Physical property measurements

The magnetic measurements were carried out on a Quantum Design Physical Property Measurement System (PPMS) using the VSM option. For the VSM measurements 9.758 mg of $CeRu_2Mg_5$ was packed in Kapton foil and attached to the sample holder rod for measuring the magnetic properties in the temperature range 3 – 305 K with magnetic flux densities up to 80 kOe.

Discussion

Crystal chemistry

So far, only the rare earth metal-rich compounds $Ce_{23}Ru_7Mg_4$ [11] and Ce_4RuMg [15] have been reported in the ternary system Ce-Ru-Mg. Both structures are built up of rigid three-dimensional networks of corner-sharing $RuCe_6$ trigonal prisms and Mg_4 tetrahedra. Although magnesium is clearly the minority component in both compounds, the magnesium clustering is remarkable. A second peculiar structural feature are comparatively short Ce–Ru distances, down to 261 pm in $Ce_{23}Ru_7Mg_4$ [11]. These Ce–Ru distances are shorter than the sum of the covalent radii of 289 pm [21]. Similar structural characteristics are observed for the new compound $CeRu_2Mg_5$ reported herein, although this compound is magnesium-rich.

The $CeRu_2Mg_5$ structure has four crystallographically independent sites. The coordination polyhedra are presented in Fig. 2. The cerium atoms have the coordination number (CN) 14 (2 Ce + 2 Ru + 10 Mg). The most intriguing feature are the extremely short Ce–Ru distances (2×) of 232 pm, which are much shorter than the sum of the covalent radii [21] of 289 pm. Such short Ce–Ru distances can only be explained by small, almost tetravalent cerium atoms, as is also evident from the magnetic data (*vide infra*). The

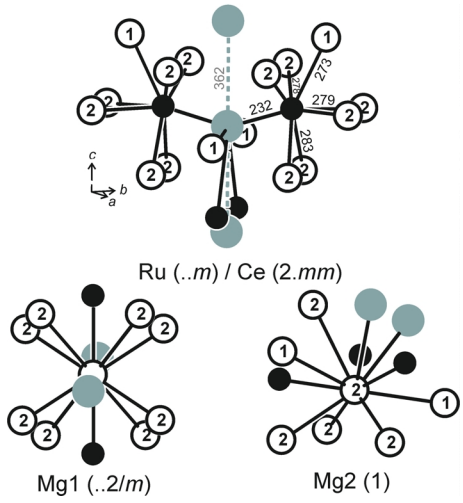

Fig. 2. Near-neighbor coordination in the structure of $CeRu_2Mg_5$. Cerium, ruthenium, and magnesium atoms are drawn as light gray, black filled, and open circles, respectively. Relevant interatomic distances and site symmetries are indicated.

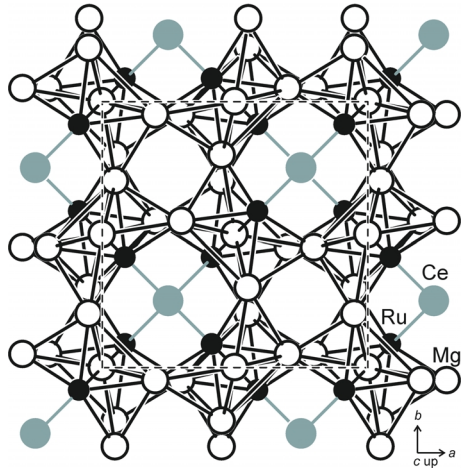

Fig. 3. Projection of the $CeRu_2Mg_5$ structure onto the *ab* plane. Cerium, ruthenium, and magnesium atoms are drawn as light gray, black filled, and open circles, respectively. The three-dimensional $[Ru_2Mg_5]$ network and the short Ce–Ru contacts are emphasized.

coordination sphere of the cerium atoms is completed by ten magnesium and two cerium atoms. The Ce–Ce distances of 362 pm are close to that in *fcc* cerium (365 pm) [22] and well above the Hill limit of 340 pm for *f* electron localization [23].

The ruthenium atoms have the smallest CN with one cerium and seven magnesium atoms in their near-neighbor environment (Fig. 2). The Ru–Mg distances range from 273 to 283 pm, slightly longer than the sum of the covalent radii of 260 pm, similar to the structure of Mg_3Ru_2 [24]. The two crystallographically independent magnesium sites have 8 (Mg1) and 6 (Mg2) magnesium neighbors at Mg–Mg distances ranging from 302 to 341 pm. Most of these Mg–Mg distances are shorter than the average Mg–Mg distance of 320 pm in *hcp* magnesium [22]. These distances compare well with the Mg–Mg distances of 313 – 315 pm in the Mg_4 tetrahedra of $Ce_{23}Ru_7Mg_4$ [11] and in the magnesium substructures of the ternary magnesium-rich compounds $LaCuMg_4$ (305 – 326 pm) [25], $TbCuMg_4$ (308 – 335 pm) [25], and $Y_5Cu_5Mg_{16}$ (300 – 342 pm) [26].

In Fig. 3 we present a projection of the $CeRu_2Mg_5$ structure onto the *ab* plane, emphasizing the Ru–Mg, Mg–Mg, and Ce–Ru interactions. Together, the ruthenium and magnesium atoms build up a rigid three-dimensional network in which the cerium atoms are located in cavities at 1/4 1/4 0.43098 and on the three symmetry-equivalent sites. As emphasized in Fig. 2, each cerium atom connects to two ruthenium atoms. On rows at 1/4 1/4 *z* and 3/4 3/4 *z* these $CeRu_2$ units are related by the four-fold srew axis 4_2. At first sight one might think of empty channels along 3/4 1/4 *z* and 1/4 3/4 *z*, however, this space is much smaller than that occupied by the neighboring cerium channels, and this part of the structure shows substantial Mg–Mg bonding.

Finally we note that most of the compounds with extremely short Ce–Ru distances crystallize in their own, singular structure type. Due to the intermediate cerium valence (almost tetravalent cerium) and the very short Ce–Ru distances no representatives with the neighboring rare earth elements can be structurally realized. To give an example, CeRuSn [6] crystallizes with a monoclinic superstructure of the CeCoAl type, while PrRuSn [27] with its orthorhombic TiNiSi-type structure contains stable trivalent praseodymium. Further investigations on $Ce_xRu_yX_z$ intermetallics are in progress in order to systematize the magnetochemical properties of these outstanding intermetallics.

Physical properties

The temperature dependence of the magnetic and the inverse magnetic susceptibility of $CeRu_2Mg_5$ is displayed in Fig. 4. The compound shows only a moderately temperature-dependent susceptibility, a typical

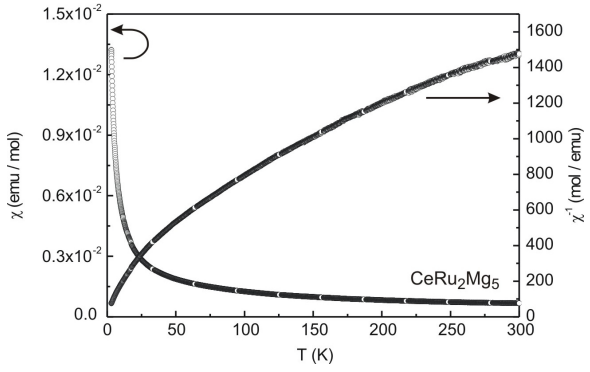

Fig. 4. Temperature dependence of the magnetic susceptibility (χ and χ^{-1} data) of $CeRu_2Mg_5$ measured at 10 kOe.

characteristic of intermediate-valent cerium compounds. The modified Curie-Weiss law $\chi = \chi_0 + C/(T - \theta_P)$ was used to fit the susceptibility in the range of 20 – 300 K. This revealed a temperature-independent term of $\chi_0 = 3.7(1) \times 10^{-4}$ emu mol^{-1}, an effective magnetic moment of $\mu_{eff} = (8C)^{1/2} = 0.9(1)\ \mu_B$ per *fu* and a paramagnetic Curie temperature of $\theta_P = -16.1(5)$ K. Since the obtained value of the effective magnetic moment is much smaller than the theoretical value of 2.54 μ_B for a free Ce^{3+} ion, an intermediate-valent cerium has to be assumed for $CeRu_2Mg_5$. Mixed-valency can also be ruled out due to the fact that only one crystallographically independent cerium site is present in the compound. Fig. 5

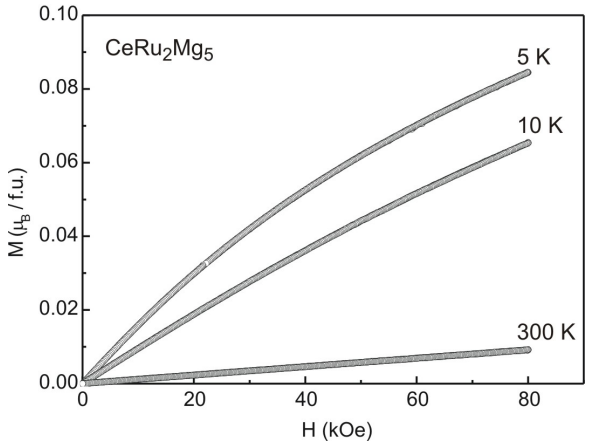

Fig. 5. Magnetization isotherms of $CeRu_2Mg_5$ measured at 5, 10, and 300 K.

displays the magnetization isotherms taken at 5, 10 and 300 K. The isotherms at 5 and 10 K show a very slight curvature, and only small magnetization values are reached at the highest measured field of 80 kOe. At 300 K the magnetization increases linearly with the external field as expected for a paramagnetic material. The magnetic behavior of $CeRu_2Mg_5$ is similar to that of $Ce_5Ru_3Al_2$ [28] and CeRuAl [13].

Acknowledgement

This work was financially supported by the Deutsche Forschungsgemeinschaft.

[1] Zh. M. Kurenbaeva, A. I. Tursina, E. V. Murashova, S. N. Nesterenko, A. V. Gribanov, Yu. D. Seropegin, H. Noël, *J. Alloys Compd.* **2007**, *442*, 86.
[2] E. V. Murashova, Zh. M. Kurenbaeva, A. I. Tursina, H. Noël, P. Rogl, A. V. Grytsiv, A. V. Gribanov, G. Giester, Yu. D. Seropegin, *J. Alloys Compd.* **2007**, *442*, 89.
[3] A. I. Tursina, Zh. M. Kurenbaeva, A. V. Gribanov, H. Noël, T. Roisnel, Y. D. Seropegin, *J. Alloys Compd.* **2007**, *442*, 100.
[4] E. V. Murashova, A. I. Tursina, Zh. M. Kurenbaeva, A. V. Gribanov, Yu. D. Seropegin, *J. Alloys Compd.* **2008**, *454*, 206.
[5] A. V. Gribanov, A. I. Tursina, A. V. Grytsiv, E. V. Murashova, N. G. Bukhan'ko, P. Rogl, Y. D. Seropegin, G. Giester, *J. Alloys Compd.* **2008**, *454*, 164.
[6] J. F. Riecken, W. Hermes, B. Chevalier, R.-D. Hoffmann, F. M. Schappacher, R. Pöttgen, *Z. Anorg. Allg. Chem.* **2007**, *633*, 1094.
[7] S. F. Matar, J. F. Riecken, B. Chevalier, R. Pöttgen, V. Eyert, *Phys. Rev. B* **2007**, *76*, 174434.
[8] R. Mishra, W. Hermes, U. Ch. Rodewald, R.-D. Hoffmann, R. Pöttgen, *Z. Anorg. Allg. Chem.* **2008**, *634*, 470.
[9] V. Eyert, E.-W. Scheidt, W. Scherer, W. Hermes, R. Pöttgen, *Phys. Rev. B* **2008**, *78*, 214420.
[10] F. Tappe, W. Hermes, M. Eul, R. Pöttgen, *Intermetallics* **2009**, *17*, 1035.
[11] S. Linsinger, M. Eul, W. Hermes, R.-D. Hoffmann, R. Pöttgen, *Z. Naturforsch.* **2009**, *64b*, 1345.
[12] T. Mishra, M. Eul, S. F. Matar, R. Pöttgen, *Z. Anorg. Allg. Chem.* **2010**, *636*, 1236.
[13] W. Hermes, S. F. Matar, R. Pöttgen, *Z. Naturforsch.* **2009**, *64b*, 901.
[14] U. Ch. Rodewald, B. Chevalier, R. Pöttgen, *J. Solid State Chem.* **2007**, *180*, 1720.
[15] S. Tuncel, B. Chevalier, S. F. Matar, R. Pöttgen, *Z. Anorg. Allg. Chem.* **2007**, *633*, 2019.

[16] R. Pöttgen, Th. Gulden, A. Simon, *GIT Labor-Fachzeitschrift* **1999**, *43*, 133.
[17] R. Pöttgen, A. Lang, R.-D. Hoffmann, B. Künnen, G. Kotzyba, R. Müllmann, B. D. Mosel, C. Rosenhahn, *Z. Kristallogr*. **1999**, *214*, 143.
[18] K. Yvon, W. Jeitschko, E. Parthé, *J. Appl. Crystallogr.* **1977**, *10*, 73.
[19] G. M. Sheldrick, SHELXS-97, Program for the Solution of Crystal Structures, University of Göttingen, Göttingen (Germany) **1997**. See also: G. M. Sheldrick, *Acta Crystallogr.* **1990**, *A46*, 467.
[20] G. M. Sheldrick, SHELXL-97, Program for the Refinement of Crystal Structures, University of Göttingen, Göttingen (Germany) **1997**. See also: G. M. Sheldrick, *Acta Crystallogr.* **2008**, *A64*, 112.
[21] J. Emsley, *The Elements*, Oxford University Press, Oxford **1999**.
[22] J. Donohue, *The Structures of the Elements*, Wiley, New York **1974**.
[23] H. H. Hill in *Plutonium and other Actinides*, (Ed.: W. N. Mines), *Nuclear Materials Series, AIME*, Vol. 17, **1970**, pp. 2.
[24] R. Pöttgen, V. Hlukhyy, A. Baranov, Yu. Grin, *Inorg. Chem.* **2008**, *47*, 6051.
[25] P. Solokha, S. De Negri, V. Pavlyuk, A. Saccone, B. Marciniak, *J. Solid State Chem*. **2007**, *180*, 3066.
[26] P. Solokha, S. De Negri, V. Pavlyuk, A. Saccone, *Solid State Sci*. **2009**, *11*, 801.
[27] J. F. Riecken, A. F. Al Alam, B. Chevalier, S. F. Matar, R. Pöttgen, *Z. Naturforsch*. **2008**, *63b*, 1062.
[28] E. V. Murashova, A. I. Tursina, N. G. Bukhanko, S. N. Nesterenko, Zh. M. Kurenbaeva, Y. D. Seropegin, H. Nöel, M. Potel, T. Roisnel, D. Kaczorowski, *Mater. Res. Bull*. **2010**, *45*, 993.